Broadband Quantum-Dot Infrared Photodetector

Wei-Hsun Lin, *Student Member, IEEE*, Chi-Che Tseng, *Student Member, IEEE*, Kuang-Ping Chao, Shu-Yen Kung, Shih-Yen Lin, *Member, IEEE*, and Meng-Chyi Wu, *Senior Member, IEEE*

***Abstract*—In this letter, we report the five-period quantum-dot infrared photodetectors (QDIPs) with a bi-stacked quantum-dot (QD) structure for a wide and relatively flat detection response ranging from 4 to 11 μm with high responsivities. The bi-stacked QD structure consists of a standard InAs QD and an InGaAs-capped InAs QD layer separated by a 50-nm GaAs barrier layer. The device exhibits a wide detection window in the range of 4–11 μm with high responsivities, which suggests that similar responsivities can be obtained for the standard QD and the InGaAs-capped QD layers in the mid-wavelength (MWIR) and long-wavelength (LWIR) infrared ranges, respectively. The results are advantageous for the development of broadband QDIPs covering MWIR and LWIR ranges based on the stacked QD structures.**

***Index Terms*—Quantum-dot infrared photodetectors (QDIPs).**

I. Introduction

INFRARED detection has been widely adopted in numerous applications such as industry, environment monitoring, medical diagnostics, and military. Among all the applications, multicolor detections are usually required. To achieve this goal, quantum-well infrared photodetectors (QWIPs) are usually adopted since the detection wavelengths of such devices could be easily manipulated by changing the quantum-well (QW) thickness or the barrier heights [1]–[3]. QWIP with broad detection wavelengths has been also reported by stacking several QW active regions with different absorption regions [3]. Compared with QWIPs, quantum-dot infrared photodetectors (QDIPs) have been reported to be of a broad detection window, a high operation temperature, and insensitive to normally incident light [4]–[6]. However, there are no reports on the QDIPs with the broad detection window covering mid-wavelength infrared [(MWIR) 3–5 μm] and long-wavelength infrared [(LWIR) 8–12 μm] ranges. The main reason responsible for this phenomenon is the difficulty of wavelength control by using the self-assembled quantum-dot (QD) structures. Although wide detection windows resulted from the QD size variation are observed for QDIPs, the detection wavelengths are limited at the MWIR range. Therefore, an even wider detection covering both MWIR and LWIR ranges is required for a single QDIP.

In this letter, a five-period QDIP with bi-stacked QD structure is investigated. The bi-stacked QD structure consists of standard 2.5 mono-layer (ML) InAs QDs and InGaAs-capped 2.0 ML InAs QDs separated by a 50-nm GaAs barrier layer. The device would exhibit a wide detection window ranging from 4 to 11 μm with high responsivities. The phenomenon is attributed to the high responsivities of the standard QD and the InGaAs-capped QD structures in the MWIR and LWIR ranges, respectively. The results have also demonstrated the possibility of broad detections covering MWIR and LWIR ranges by using the stacked QD structures without degrading the device performance.

II. Experiments

The samples investigated in this letter are grown on (100)-oriented semi-insulated GaAs substrates using a Riber Compact 21 solid source molecular beam epitaxy (MBE) system. For all the samples, 600- and 300-nm GaAs layers with n-type doping 2×10^{18} cm^{-3} are grown as bottom and top contact layers. Three samples with 1) ten-period standard 2.5 ML InAs–GaAs QDs, 2) ten-period $In_{0.15}Ga_{0.85}As$-capped 2.0 ML InAs QDs, and 3) five-period bi-stacked 2.5 ML InAs–GaAs and $In_{0.15}Ga_{0.85}As$-capped 2.0 ML InAs QDs were prepared, which are referred as Devices A, B, and C, respectively. The GaAs barrier thicknesses are 50 and 42 nm for the standard and InGaAs-capped QD structures, respectively. For Device C, the growth sequence is standard QDs following by the InGaAs-capped QD structure. Standard photolithography and chemical wet etching were processed to define to the devices with 100×100 μm^2 mesas. The spectral responses for the device were measured under an edge-coupling scheme. The positive and negative polarities were defined to the voltages applied to the top of the device. The measurement system for spectral response consisted of a Perkin Element spectrum 100 Fourier transform infrared (FTIR) coupling with a Janis cryostat and a current preamplifier [6].

III. Results and Discussion

The 10 K spectral responses of Device A at ± 2.2 V are shown in Fig. 1. As shown in this figure, a wide detection window ranging from 4 to 8 μm is observed for the device, which is frequently observed for standard QDIPs [6]. The symmetric high responsivity of Device A under positive and negative biases has also demonstrated the optimized growth conditions

Manuscript received December 18, 2009; revised March 29, 2010; accepted April 09, 2010. Date of publication April 19, 2010; date of current version June 09, 2010. This work was supported in part by the National Science Council, Taiwan, under the Grant NSC 98-2221-E-001-001 and Grant NSC 99-2911-I-001-010.

W.-H. Lin, K.-P. Chao, and S.-Y. Kung are with the Institute of Electronics Engineering, National Tsing Hua University, Hsinchu 300, Taiwan (e-mail: twogenius2000@yahoo.com.tw; espn777a@hotmail.com; k3535604@hotmail.com).

C.-C. Tseng is with the Institute of Photoics Technologies, National Tsing Hua University, Hsinchu 300, Taiwan (e-mail: m93530100@gmail.com).

S.-Y. Lin is with the Research Center for Applied Sciences, Academia Sinica, Taipei 11529, Taiwan, with the Department of Photonics, National Chiao-Tung University, Hsinchu 300, Taiwan, and also with the Institute of Optoelectronic Sciences, National Taiwan Ocean University, Keelung 20224, Taiwan (e-mail: shihyen@gate.sinica.edu.tw).

M.-C. Wu is with the Institute of Electronics Engineering, National Tsing Hua University, Hsinchu 300, Taiwan, and also with the Institute of Photoics Technologies, National Tsing Hua University, Hsinchu 300, Taiwan (e-mail: mcwu@ee.nthu.edu.tw).

Digital Object Identifier 10.1109/LPT.2010.2048425

1041-1135/$26.00 © 2010 IEEE

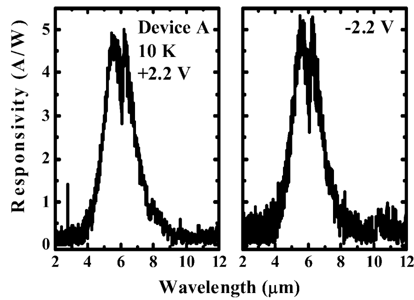

Fig. 1. The 10 K spectral responses of Device A at ±2.2 V.

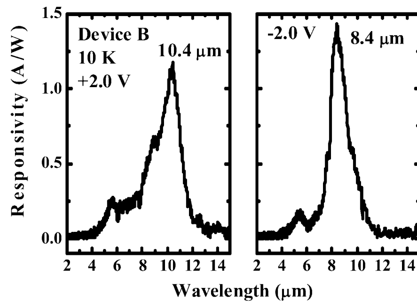

Fig. 2. The 10 K spectral responses of Device B at ±2.0 V.

for this QDIP sample. However, difficulties still remain for extending the detection wavelength of QDIPs to the LWIR range. To achieve this goal, reports regarding the InAs QDs embedded in the InGaAs quantum-well (DWELL) structure have been proposed [7], [8]. The devices have exhibited the LWIR detection. However, for such devices, an additional InGaAs layer prior to the QD growth is always required to achieve the devices operated at longer detection wavelengths [8]. With the more complicated structures, device parameter optimization such as the underlying InGaAs thickness and growth conditions would be required to achieve high device performance and long detection wavelengths. Therefore, a simpler InGaAs-capped QD structure with reduced InAs coverage has been reported [9]. The design of such a structure is to upraise the energy levels of the QD structures instead of depressing the energy level of the wetting layer.

The 10 K spectral responses of Device B at ±2.0 V are shown in Fig. 2. The peak responses at 10.4 and 8.4 μm are observed for this device under positive and negative biases, respectively. As discussed in our previous report, the asymmetric peak responses of Device B are attributed to the strong Stark effect resulted from the asymmetric InGaAs-capped QD structure [9]. An inspection of this figure also reveals that Device B has a high responsivity of up to 1.0 A/W, which demonstrates the high epitaxial quality of the InGaAs-capped structure. The results have also confirmed that by using the relatively simple InGaAs-capped QD structure with reduced InAs coverage, high responsivities and LWIR detections could both be achieved. With the device performance of standard and InGaAs-capped QDIPs, a straightforward approach to achieve broadband QDIPs is to stack the two structures into one device. However, according to our previous report, most of the photocurrents of QDIPs come from the QD structure near the cathode side of the device [10]. Therefore, for

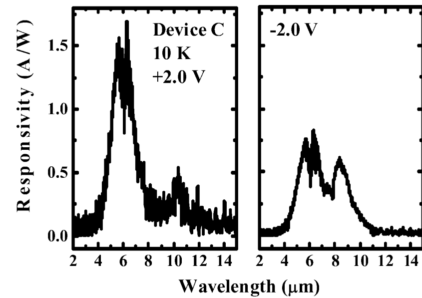

Fig. 3. The 10 K spectral responses of Device C at ±2.0 V.

a device with two separate QD regions with different detection wavelengths, the result would be a voltage-tunable two-color QDIP as discussed elsewhere [10]. In this case, a device structure with bi-stacked standard and InGaAs-capped QD layers like Device C would be necessary to achieve broadband detections.

The 10 K spectral responses of Device C at ±2.0 V are shown in Fig. 3. When this device is positively biased, two response peaks at ~6 and ~10 μm are observed. On the other hand, when the device is operated under negative biases, a broad detection window in the range of 4–11 μm is observed. It is obvious that the response of Device C is the combination of Devices A and B under different bias polarities. In the bi-stacked QD structure, the standard 2.5 ML InAs–GaAs QDs would contribute the photocurrents in the MWIR range at either the positive or negative bias. In addition, the InGaAs-capped QDs would contribute the ~10.4 and ~8.4 μm responses at positive and negative biases, respectively. In this case, two distinct responses at ~6 and ~10 μm are observed for Device C at ±2.0 V and a broad response ranging from 4 to 11 μm is observed at −2.0 V. The results of Device C have already demonstrated the application of the bi-stacked QD structure in the development of broadband QDIPs.

The other issue remaining is the request of flat response curves of broad QDIPs in the whole response range. Since Device A has exhibited higher responsivities than Device B, a similar phenomenon is also observed for Device C that the MWIR response is still higher than the LWIR response. To further investigate this phenomenon, the 10 K MWIR and LWIR peak responsivities of Device C under different applied voltages are shown in Fig. 4(a). When the device is under positive biases, the MWIR response would be stronger than the LWIR response at high applied voltages. To explain this phenomenon, schematic band diagrams of the bi-stacked QD structure near the cathode terminal under positive and negative biases are shown in Fig. 4(b). Since most of the photocurrent comes from the QD structures near the cathode terminal, the two QD structures discussed in the band diagrams under positive and negative biases are close to bottom and top contact layers, respectively [10]. As shown in the figure, there are four states to be observed in the bi-stacked QD structure, which are the ground and the first excited states of the QDs $E_{\mathrm{QD},0}$ and $E_{\mathrm{QD},1}$, the QW ground state in the InGaAs layer E_{InGaAs}, and the wetting layer state E_{WL} [9]–[11]. When the device is under positive biases, because the standard QDs of the bi-stacked structure are closer to the cathode side, a longer

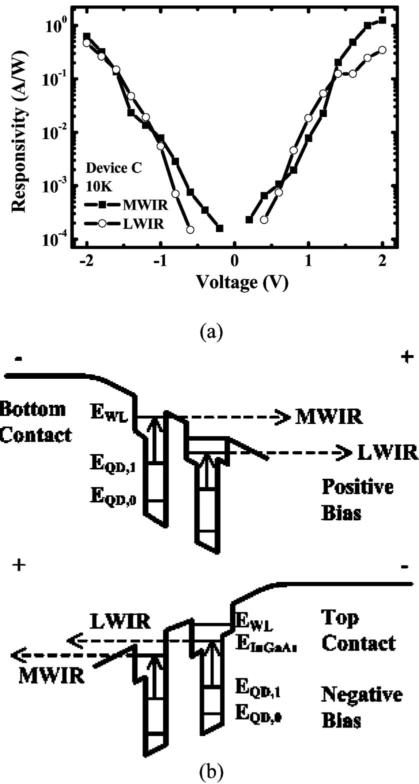

Fig. 4. (a) The 10 K MWIR and LWIR peak responsivities of Device C under different applied voltages and (b) schematic band diagrams of the bi-stacked QD structure near the cathode terminal under positive and negative biases.

traveling path in the device structure for the photoexcited electrons responsible for the MWIR responses is obtained. Considering the avalanche process is involved for QDIPs at high applied voltages, a more pronounced avalanche process would take place for the electrons coming out from the standard QDs such that the much higher MWIR response of Device C under high positive biases is observed. On the contrary, when Device C is under negative biases, a longer traveling path is experienced by the photoexcited electrons responsible for the LWIR responses. In this case, the more pronounced avalanche process of the electrons coming out from the InGaAs-capped QDs would be observed. This phenomenon would compensate the intrinsically lower responsivity of the LWIR response such that similar MWIR and LWIR responsivities are observed for Device C under negative biases. This is the main reason why a broad and relatively flat response curve could be observed for Device C under negative biases.

IV. Conclusion

We have demonstrated the five-period QDIP with bi-stacked QD structure for a wide and relatively flat detection response ranging from 4 to 11 μm with high responsivities. The bi-stacked QD structure consists of standard InAs QDs and InGaAs-capped InAs QDs separated by a 50-nm GaAs barrier layer. The device has exhibited a wide detection window ranging from 4 to 11 μm with high responsivities under negative biases. To extend the detection wavelengths and obtain a flatter response curve, a tri-stacked QD structure with a standard InAs QDs sandwiched by two different InGaAs-capped QDs may be necessary for further investigation in the future.

References

[1] B. F. Levine, G. Hasnain, C. G. Bethea, and N. Chand, "Broadband 8–12 μm high-sensitivity GaAs quantum well infrared photodetector," *Appl. Phys. Lett.*, vol. 54, pp. 2704–2706, Jun. 1989.

[2] S. V. Bandara, S. D. Gunapala, J. K. Liu, E. M. Luong, J. M. Mumolo, W. Hong, D. K. Sengupta, and M. J. McKelvey, "10–16 μm Broadband quantum well infrared photodetector," *Appl. Phys. Lett.*, vol. 72, pp. 2427–2429, May 1998.

[3] S. V. Bandara, S. D. Gunapala, J. K. Liu, S. B. Rafol, C. J. Hill, D. Z.-Y. Ting, J. M. Mumolo, T. Q. Trinh, J. M. Fastenau, and A. W. K. Liu, "Tuning and tailoring of broadband quantum-well infrared photodetector responsivity spectrum," *Appl. Phys. Lett.*, vol. 86, pp. 151104–151106, Apr. 2005.

[4] S. Y. Lin, Y. R. Tsai, and S. C. Lee, "High-performance InAs/GaAs quantum-dot infrared photodetector with single-sided $Al_{0.3}Ga_{0.7}As$ blocking layer," *Appl. Phys. Lett.*, vol. 78, pp. 2784–2786, Apr. 2001.

[5] S. F. Tang, S. Y. Lin, and S. C. Lee, "Near-room-temperature operation of an InAs/GaAs quantum-dot infrared photodetector," *Appl. Phys. Lett.*, vol. 78, pp. 2428–2430, Apr. 2001.

[6] S. T. Chou, M. C. Wu, S. Y. Lin, and J. Y. Chi, "The influence of doping density on the normal incident absorption of quantum-dot infrared photodetectors," *Appl. Phys. Lett.*, vol. 88, pp. 173511–173513, Apr. 2006.

[7] S. D. Gunapala, S. V. Bandara, C. J. Hill, D. Z. Ting, J. K. Liu, S. B. Rafol, E. R. Blazejewski, J. M. Mumolo, S. A. Keo, S. Krishna, Y. C. Chang, and C. A. Shott, "Long-wavelength infrared (LWIR) quantum dot infrared photodetector (QDIP) focal plane array," *Proc. SPIE*, vol. 6206, p. 62060J, 2006.

[8] S. Raghavan, D. Forman, P. Hill, N. R. Weisse-Bernstein, G. von Winckel, P. Rotella, S. Krishna, S. W. Kennerly, and J. W. Little, "Normal-incidence $InAs/In_{0.15}Ga_{0.85}As$ quantum dots-in-a-well detector operating in the long-wave infrared atmospheric window (8–12 μm)," *J. Appl. Phys.*, vol. 96, pp. 1036–1039, Jul. 2004.

[9] W. H. Lin, C. C. Tseng, K. P. Chao, S. C. Mai, S. Y. Lin, and M. C. Wu, "InGaAs-Capped InAs/GaAs quantum-dot infrared photodetectors operating in the long-wavelength infrared range," *IEEE Photon. Technol. Lett.*, vol. 21, no. 18, pp. 1332–1334, Sep. 15, 2009.

[10] S. Y. Lin, W. H. Lin, C. C. Tseng, K. P. Chao, and S. C. Mai, "Voltage-tunable two-color quantum-dot infrared photodetectors," *Appl. Phys. Lett.*, vol. 95, pp. 123504–123506, Sep. 2009.

[11] C. C. Tseng, S. T. Chou, S. Y. Lin, C. N. Chen, W. H. Lin, Y. H. Chen, T. H. Chung, and M. C. Wu, "The transition mechanisms of a ten-Period InAs/GaAs quantum-dot infrared photodetector," *J. Vac. Sci. Technol. B*, vol. 26, pp. 1831–1833, Nov./Dec. 2008.